Symmetric-to-Asymmetric Transition in Triblock Copolymer-Homopolymer Blends

P. Falus,[1,2] H. Xiang,[3] M. A. Borthwick,[2] T. P. Russell,[3] and S. G. J. Mochrie[1]

[1]*Department of Physics, Yale University, New Haven, Connecticut 06511 USA*

[2]*Department of Physics, Massachusetts Institute of Technology, Cambridge, Massachusetts 02139 USA*

[3]*Polymer Science and Engineering Department, University of Massachusetts, Amherst, Massachusetts 01002 USA*

(Received 9 June 2004; published 27 September 2004)

In blends of a symmetric poly(styrene-ethylene/butylene-styrene) tri-block-copolymer with a polystyrene homopolymer, small-angle x-ray scattering and cryotransmission electron microscopy measurements reveal a microstructure consisting of a disordered arrangement of poly(ethylene/butylene) membranes suspended in polystyrene. For triblock volume fractions less than 0.22, the membranes form an asymmetric sponge or L_4 phase, consisting predominantly of equilibrium vesicles. For volume fractions greater than 0.22, they form a symmetric sponge-phase (L_3 phase), separated from the L_4 phase by a first-order transition.

DOI: 10.1103/PhysRevLett.93.145701 PACS numbers: 64.70.Ja, 61.25.Hq, 83.80.Uv

Amphiphilic molecules can self-organize to create complex fluids with characteristic length scales in the 10–100 nm range. A special advantage of polymeric systems [1–6] for basic studies, in comparison to those involving small molecules, is that, in many cases, polymer behavior can be accurately described by self-consistent field theory (SCFT), based on a few known parameters. Therefore, studies of polymer amphiphiles promise an essentially first-principles understanding of complex fluid phase behavior and structure [7,8].

It is therefore surprising that one of the most intriguing phases found in small-molecule complex fluids has not yet been fully characterized in block copolymer systems, namely, the L_3 symmetric sponge-phase [9–14]. The L_3 phase appears in two-component amphiphile-solvent mixtures in which the amphiphiles self-assemble into an extended, random, multiply-connected membrane. Several theoretical approaches have been aimed at understanding the stability of the L_3 phase, relative to a lamellar (L_α) phase or a vesicle (L_4) phase, including membrane-based models [15–21], microscopic lattice models [22,23], and Landau-Ginsburg-type theories. Nevertheless, key issues remain. These include the importance of anharmonic contributions to the membrane bending free energy, the effect of possible length-scale-dependent renormalization of the membrane elastic constants, and the role of the membrane's Gaussian curvature energy.

A particularly interesting aspect of the sponge-phase is the possibility of a "symmetric-to-asymmetric" (S-to-A) transition: The sponge-phase membrane divides space into two distinct solvent volumes which can be labeled "inside" (I) and "outside" (O). Either the I and O volumes are equivalent, which corresponds to theL_3 phase, or the I-O symmetry is broken, corresponding to the asymmetric sponge (A) phase, which actually has the same symmetry as an L_4 phase. The S-to-A transition is analogous to the ordering transition of Ising spins. However, unlike neutron scattering from domains of up and down spins, scattering experiments do not have direct access to fluctuations in the I-O order parameter, since there is no I-O contrast. Instead, any scattering originates solely in the contrast between membrane and solvent. Nevertheless, elegant theoretical descriptions of the sponge-phase scattering are predicated on coupling between the amphiphile density and I-O order parameter fluctuations [11,25].

Here we report small-angle–x-ray-scattering (SAXS) and cryotransmission electron microscopy (CTEM) results for blends of a poly(styrene-ethylene/butylene-styrene) symmetric tri-block-copolymer (PSEBS) with a short-chain polystyrene homopolymer (PS) versus composition and temperature. These measurements reveal the existence of polymeric L_3 and L_4 phases [26] and, for the first time, a first-order S-to-A transition in a block-copolymer-homopolymer blend. In addition, the SAXS measurements permit a systematic comparison with the theoretical structure factor given in Ref. [25]. From the point of view of gaining a basic understanding of complex fluid phases, our results are significant because the tractability of microscopic calculations for polymers should permit accurate determination of key membrane parameters using SCFT.

We used PSEBS symmetric tri-block-copolymer [27] with $M_w = 80.7$ kg/mole and $M_w/M_n = 1.07$ and an ethylene/butylene midblock fraction of 0.70, and PS homopolymer [28] with $M_w = 4.82$ kg/mole and $M_w/M_n = 1.11$. Samples were prepared by codissolving these materials in toluene, filtering the solution to 0.02 μm, followed by precipitation into cold propanol. They were then annealed under vacuum at 160 °C for at least a week prior to the SAXS measurements, which were performed at beam line 8-ID at the Advanced Photon Source (APS). Scattered x-rays were collected by a charge-coupled device-based detector (CCD). Additional measurements were carried out at beam line X22A at the National Synchrotron Light Source (NSLS) using a point detector.

For the CTEM, samples were also annealed under vacuum at 160 °C for seven days. They were then microtomed at −100 °C, and stained with RuO_4.

The time- and circularly-averaged x-ray scattering cross-sections (Σ) are displayed in Fig. 1(a) for wave vectors (Q) from 0.02 to 1.3 nm^{-1} for samples with PSEBS volume fractions of $\phi = 0.15$, 0.19, 0.30 and 0.40. An important feature of the profiles shown, and of data obtained for all volume fractions studied between $\phi = 0.07$ and $\phi = 0.43$, is the presence of prominent intensity oscillations. The locations of the oscillation minima, occuring at integer multiples of 0.32 nm^{-1}, require a microstructure that consists predominantly of membranes with a thickness of $d \simeq 19$ nm.

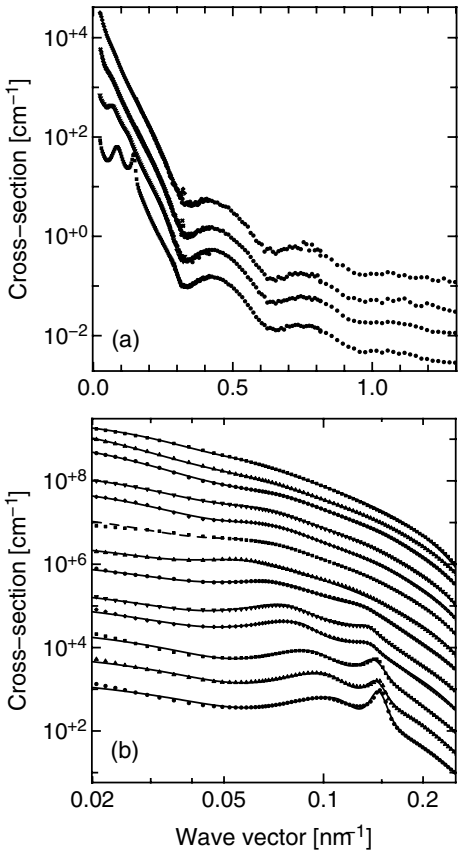

FIG. 1. X-ray scattering cross-sections for PSEBS-PS blends *vs.* wave vector. (a) Data for, from top to bottom, $\phi = 0.15$, 0.19, 0.30 and 0.40 for wave vectors from 0.02 to 1.3 nm^{-1}. For clarity, these profiles have been multiplied by 5^3, 5^2, 5, and 1, respectively. (b) Data for $\phi = 0.07$, 0.11, 0.15, 0.17, 0.19, 0.22, 0.25, 0.28, 0.31, 0.34, 0.37, 0.40 and 0.43, plotted from 0.02 to 0.2 nm^{-1} on a log-log scale. These profiles have been multiplied by 3^{12}, 3^{11}, 3^{10}, 3^9, 3^8, 3^7, 3^6, 3^5, 3^4, 3^3, 3^2, 3, and 1, respectively. Solid lines correspond to the model discussed in the text. The dashed line through the profile for $\phi = 0.22$ corresponds to coexistence of 40% $\phi = 0.25$-volume fraction material with 60% $\phi = 0.19$-volume fraction material.

Figure 1(b) shows SAXS profiles for PSEBS volume fractions of $\phi = 0.07$, 0.11, 0.15, 0.17, 0.19, 0.22, 0.25, 0.28, 0.31, 0.34, 0.37, 0.40, and 0.43, for wave vectors between 0.02 and 0.25 nm^{-1} on a log-log scale, highlighting the small wave vector region. These data were obtained at 160 °C, but profiles obtained throughout the temperature range between 120 and 200 °C are similar. At $\phi = 0.07$, the intensity is peaked at zero wave vector and decreases smoothly with increasing wave vector. For ϕ between 0.11 and 0.19, the peak at zero wave vector remains, although with decreasing intensity. In addition, throughout this range, the data now show a shoulder, occurring at about 0.065 nm^{-1}, approximately independent of ϕ. For $\phi = 0.22$, the profile can be conceived as an average of that obtained for $\phi = 0.19$ and that obtained at $\phi = 0.25$. At $\phi = 0.25$, the shoulder apparent at lower PSEBS volume fractions has been replaced by a peak, now occurring at a distinctly smaller wave vector of about 0.055 nm^{-1}. For volume fractions increasing beyond 0.25, the forward scattering becomes weaker, while the peak becomes stronger and progressively moves to larger wave vectors, varying linearly with ϕ (see Fig. 3(a)). The distinct behavior of the shoulder/peak below and above $\phi = 0.22$ suggest the existence of different phases above and below $\phi = 0.22$. Consistent with this interpretation is that the data for $\phi = 0.22$ are quite well-described by a model line shape that is a weighted sum of the line shapes for $\phi = 0.19$ (40%) and $\phi = 0.25$ (60%), corresponding to two-phase coexistence, which is shown as the dashed line in Fig. 1(b).

Evidently, an additional, narrow peak appears and grows at somewhat larger wave vectors for volume fractions increasing beyond 0.28. CCD images (not shown) reveal that, in contrast to the remainder of the scattering, which is azimuthally symmetric, this component varies as a function of azimuthal scattering angle, implying that it originates within differently-oriented grains of an L_α phase. This component aside, the existence of a membrane-based phase showing an isotropic scattering profile with a peak at zero wave vector and a broad peak at nonzero wave vector with a peak position that varies linearly with ϕ is characteristic of a sponge-phase [13,14]. On this basis, we propose that PSEBS-PS forms a stable L_3 phase for ϕ from about 0.22 to at least 0.43. There is no precedent in L_3 phases for the weak ϕ dependence of the shoulder position for $\phi \leq 0.19$. Therefore, in view of the theoretical prediction of an *S*-to-*A* transition with decreasing amphiphile volume fraction, we are led to identify the abrupt change in behavior as an *S*-to-*A* transition with the emergence of an *A* phase for low PSEBS volume fractions.

To test this assignment, we performed CTEM measurements on samples with $\phi = 0.07$ and $\phi = 0.19$. Representative TEM images are shown in Fig. 2. All images confirm the existence of membranes. The mem-

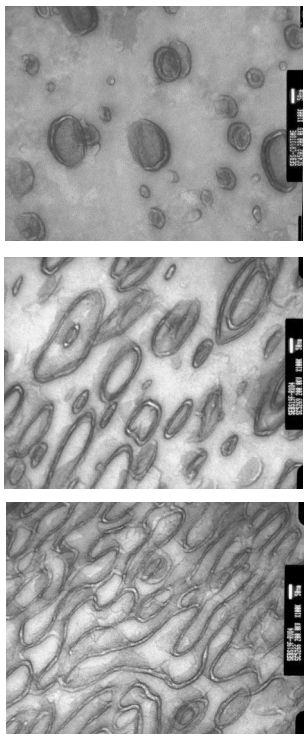

FIG. 2. CTEM images with a magnification of 10^5 of PSEBS-PS samples with $\phi = 0.07$ (top) and $\phi = 0.19$, showing L_3 (center) and L_4 (bottom) regions. The white bar in each image is 50 nm.

brane surfaces are strongly RuO_4-stained, yielding a bilayer appearance. The separation between these bilayer surfaces is comparable to the ethylene/butylene membrane width determined by SAXS. For $\phi = 0.07$ (top), a number of membrane loops are apparent, with a broad distribution of diameters extending from about 50 to about 300 nm. There are also a number of small (20–30 nm-diameter) micelles without a PS interior. It is natural to interpret this image as showing isolated vesicles and micelles, firmly fixing this volume fraction within an A (L_4) phase. The center image, obtained for $\phi = 0.19$, is representative of about 95% of this sample and also shows membrane loops with a broad distribution of sizes, but it includes larger loops and a higher density of loops. Interestingly, there are also nested configurations, where smaller loops lie within larger loops, as may be expected for an A phase, not too far from the S-to-A transition. The bottom image, also obtained for $\phi = 0.19$, corresponds to about 5% of the sample. This image depicts a multiply-connected morphology, for which I and O cannot be distinguished, as expected for an L_3 phase. Evidently, the $\phi = 0.19$ sample lies near, but just within, the boundary of a two-phase coexistence region and shows both L_4 and L_3 domains.

In view of what is observed in small-molecule systems [10] and predicted theoretically [17,19,20], it is not surprising to find an L_α phase in close proximity to an L_3 phase. What may be surprising is to observe L_3-L_α coexistence over a relatively wide range of ϕ, within which the L_3 phase peak position evolves versus ϕ. Gibbs' Phase Rule forbids such behavior in a strictly two-component blend in thermal equilibrium. However, our polymer materials are slightly polydisperse, so that two-phase coexistence can involve fractionation and an evolution of the coexisting phases with ϕ [29]. Analogous behavior is seen, for example, at isotropic-nematic coexistence in a system of polydisperse hard rods [30].

To quantify the PSEBS-PS sponge-phase, we have fit the SAXS profiles to the model sponge-phase structure factor given in Ref. [25], modified to account for the nonzero membrane thickness (d). The possible fitting parameters for the L_3 phase are k, ξ, ξ_ρ, γ_1, γ_2, γ_3, and d, where ξ is the correlation length of the I-O order parameter, k is the modulation wave vector for the I-O order parameter, ξ_ρ is the amphiphile correlation length, and γ_1, γ_2, and γ_3 characterize the coupling between the I-O order parameter and the amphiphile density. Additional parameters describe the L_α phase scattering. In their original paper, Gompper and Schick [25] showed good agreement between the scattering from the L_3 phase of sodium bis(2-ethylhexyl)sulfosuccinate-brine-brine [13] and their model with $\gamma_1 = 0$. Motivated by this observation, and the otherwise large number of fitting parameters, we have fixed γ_1 to zero for all of our fits. It may be shown that for $\gamma_1 = 0$, the model of Ref. [25] is appropriate for both the S and A phases [21]. The model profiles so-obtained, shown as the solid lines in Fig. 1, provide an excellent description of the SAXS data for all volume fractions studied, supporting the validity of the coupled-order-parameter description. The best-fit results for the I-O wave vector (k) are shown in Fig. 3(a) versus ϕ for 120, 160, and 200 °C. Within the L_3 phase, k indeed varies linearly with ϕ, while in the A phase, k is nearly independent of ϕ.

The correlation lengths (ξ and ξ_ρ) are shown versus SEBS volume fraction in Fig. 3(b), Evidently, the fits permit substantial variations in these quantities. This is because of the large number of fitting parameters remaining, even with γ_1 set to zero. Nevertheless, we see from Fig. 3(b) that ξ is about 90 nm throughout the A phase, and varies from about 80 nm at $\phi = 0.25$ to about 150 nm at $\phi = 0.43$ in the L_3 phase. The amphiphile correlation length ξ_ρ is considerably smaller than ξ, but it varies significantly from about 25 nm at lower ϕ to about 7 nm at $\phi = 0.43$. A similar behavior emerged in Refs. [14,31]. Finally, the coupling constants (γ_2 and γ_3) are displayed in Fig. 3(c). The model scattering intensity depends solely on the relative sign of γ_2 and γ_3. We chose γ_3 to be positive, yielding negative values of γ_2. In Ref. [31] it is shown that within the context of microscopic lattice models, γ_3/γ_2 should be negative, consistent with our result.

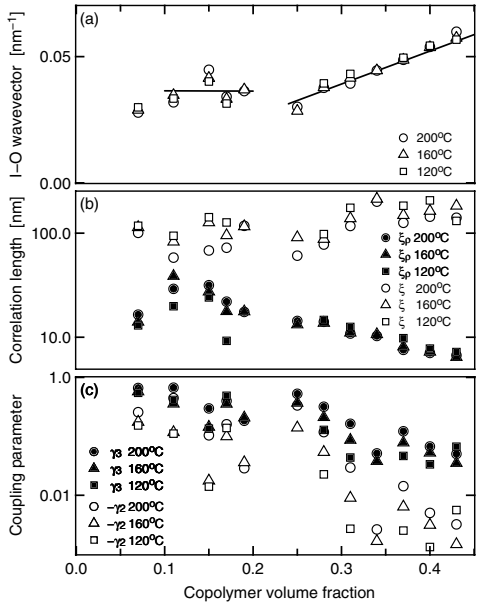

FIG. 3. Fitting parameters *vs.* PSEBS volume fraction. (a) I-O wave vector (k) for 160, 180 and 200 °C. (b) I-O correlation length (ξ), shown as solid squares, triangles, and circles for 120, 160, and 200 °C, respectively, and amphiphile density correlation length (ξ_ρ), shown as open squares, triangles, and circles for 120, 160, and 200 °C, respectively. (c) Coupling parameters: γ_3 is shown as solid squares, triangles, and circles for 120, 160, and 200 °C, respectively, and $-\gamma_2$ is shown as open squares, triangles, and circles for 120, 160, and 200 °C, respectively.

In conclusion, our collected SAXS and CTEM measurements convincingly reveal the existence of two membrane-based, equilibrium phases — a symmetric sponge-phase (L_3 phase) and an asymmetric sponge or vesicle phase (L_4 phase) — in a tri-block-copolymer-homopolymer blend, separated by a first-order S-to-A transition. This is significant from the point of view of gaining a basic understanding of these complex fluid phases, because the tractability of microscopic calculations for polymers should permit accurate determination of κ, $\bar{\kappa}$, *etc.* using SCFT. For example, Ref. [20] and Ref. [19] permit an S-to-A (L_3-to-L_4) transition only when both $|\bar{\kappa} + 10\kappa/9|$ is less than $O(k_BT)$ and the structural length scale is $O[a \exp(4\pi\kappa/3k_BT)]$ with a a microscopic length. SCFT calculations of κ and $\bar{\kappa}$ for the membranes in PS-PSEBS would provide a very interesting test of these predictions. This work also introduces two new phases to the repertoire realized in two-component block-copolymer-homopolymer blends.

We thank L. Golubovic, M. Kolarchyck, D. Lumma, L. Lurio, S. Narayanan, and A. Sandy for valuable discussions, and H. Gibson for technical assistance. This work was suppported by the NSF via DMR 0071755, and by the NSF-supported MRSEC at the University of Massachusetts, Amherst. APS and NSLS are supported by the US DOE.

[1] S. T. Milner and T. A. Witten, J. Phys. (France) **49**, 1951 (1988).
[2] Z. G. Wang and S. A. Safran, J. Phys. (France) **51**, 185 (1990).
[3] M. W. Matsen and M. Schick, Macromolecules **26**, 3878 (1993).
[4] F. S. Bates, W. W. Maurer, P. M. Lipic, M. A. Hillmyer, K. Almdal, K. Mortensen, G. H. Fredrickson, and T. P. Lodge, Phys. Rev. Lett. **79**, 849 (1997).
[5] H. S. Jeon, J. H. Lee, and N. P. Balsara, Phys. Rev. Lett. **79**, 3274 (1997).
[6] J. H. Lee, M. L. Ruegg, N. P. Balsara, Y. Zhu, S. P. Gido, R. Krishnamoorti, and M.-H. Kim, Macromolecules **36**, 6537 (2003).
[7] G. H. Fredrickson and F. S. Bates, Eur. Phys. J. B **1**, 71 (1998).
[8] M. W. Matsen, J. Chem. Phys. **110**, 4658 (1999).
[9] G. Porte, J. Marignan, P. Bassereau, and R. May, J. Physique **49**, 511 (1988).
[10] R. Strey, R. Schoemacker, D. Roux, F. Frederic, and U. Olsson, J. Chem. Soc., Faraday Trans. **86**, 2253 (1990).
[11] D. Roux, M. E. Cates, U. Olsson, R. C. Ball, F. Nallet, and A. M. Bellocq, Europhys. Lett. **9**, 229 (1990).
[12] C. Coulon, D. Roux, and A. M. Bellocq, Phys. Rev. Lett. **66**, 1709 (1991).
[13] M. Skouri, J. Marignan, J. Appell, and G. Porte, J. Phys. II (France) **1**, 1121 (1991).
[14] N. Lei, C. R. Safinya, D. Roux, and K. S. Liang, Phys. Rev. E **56**, 608 (1997).
[15] M. E. Cates, D. Roux, D. Andelman, S. T. Milner, and S. A. Safran, Europhys. Lett. **5**, 733 (1988).
[16] D. Anderson, H. Wennerstrom, and U. Olsson,J. Phys. Chem. **93**, 4243 (1989).
[17] L. Golubovic and T. C. Lubensky, Phys. Rev. A **41**, 4343 (1990).
[18] H. Wennerstrom and U. Olsson, Langmuir **9**, 365 (1991).
[19] D. C. Morse, Phys. Rev. E **50**, R2423 (1994).
[20] L. Golubovic, Phys. Rev. E **50**, R2419 (1994).
[21] P. Pieruschka and S. A. Safran, Europhys. Lett. **31**, 207 (1995).
[22] B. Widom, J. Chem. Phys. **84**, 6943 (1986).
[23] G. Gompper and M. Schick, Phys. Rev. B **41**, 9148 (1990).
[24] D. Roux, C. Coulon, and M. E. Cates, J. Phys. Chem. **96**, 4174 (1992).
[25] G. Gompper and M. Schick, Phys. Rev. E **49**, 1478 (1994).
[26] J. H. Laurer, J. C. Fung, J. W. Sedat, S. D. Smith, J. Samseth, K. Mortensen, D. A. Agard, and R. J. Spontak, Langmuir **13**, 2177 (1997).
[27] Kraton G1652, Shell International, Houston, TX, U.S.A.
[28] Polymer Source Inc., Dorval, QC, Canada.
[29] R. M. L. Evans, D. J. Fairhurst, and W. C. K. Poon, Phys. Rev. Lett. **81**, 1326 (1998).
[30] P. A. Buining and H. N. W. Lekkerkerker, J. Phys. Chem. **97**, 11510 (1993).
[31] H. Endo, M. Mihailescu, M. Monkenbusch, J. Allgaier, G. Gompper, D. Richter, B. Jakobs, T. Sottmann, R. Strey, and I. Grillo, J. Chem. Phys. **115**, 580 (2001).